Original Article

Bioactive mesoporous wollastonite particles for bone tissue engineering

Journal of Tissue Engineering
Volume 7: 1–6
© The Author(s) 2016
Reprints and permissions:
sagepub.co.uk/journalsPermissions.nav
DOI: 10.1177/2041731416680319
tej.sagepub.com
SAGE

S Saravanan[1,2] and Nagarajan Selvamurugan[1]

Abstract

The current investigation was aimed at identifying the role of mesoporous wollastonite particles on the healing of rat tibial bone defect. The bone defect was created with a 3-mm-diameter dental drill, and it was filled with mesoporous wollastonite particles. After second and fourth weeks of filling treatments, it was found that mesoporous wollastonite particles promoted bone formation as evidenced by X-ray, histological, scanning electron microscope, and energy-dispersive spectra studies. X-ray study showed the closure of drill hole as seen by high-dense radio-opacity image. Histological analysis depicted the deposition of collagen in the bone defect area in response to mesoporous wollastonite particles' treatment. Scanning electron microscope–energy-dispersive spectra analyses of the sectioned implants also identified the deposition of apatite by these particles. Thus, our results suggested that mesoporous wollastonite particles have bioactive properties, and they can be used as a suitable filling material for promotion of bone formation in vivo.

Keywords

Rice straw ash, mesoporous wollastonite, calcium silicate, bone defect

Date received: 14 August 2016; accepted: 1 November 2016

Introduction

Bone is a highly vascularized connective tissue and is under continuous remodeling process to maintain homoeostasis and repair microtraumas caused by several clinical conditions.[1] However, under critical conditions, the physiological process depends on external augmentation including auxiliary therapies such as surgeries, bone implantation procedures, and use of biomaterials. Calcium silicate ($CaSiO_3$)–based ceramics have been widely implicated in treating bone defect, as supported by its widespread use in the field of orthopedics. $CaSiO_3$ ceramics possess bioactivity and biodegradability suited for bone tissue engineering applications.[2–6]

$CaSiO_3$ ceramics have been shown to promote osteoblasts' cell attachment, proliferation, and differentiation.[3,7–9] $CaSiO_3$-based cements were able to induce the formation of apatite when immersed in simulated body fluids (SBFs), thus indicating their bioactivity properties.[10–13] Mesoporous $CaSiO_3$ or wollastonite (m-WS) materials have been widely used for bone tissue regeneration, and the hierarchized pores in mesoporous materials facilitate improved apatite deposition and protein adsorption, a pre-requisite for cell interaction allowing their candidature over other non-mesoporous materials for bone tissue regeneration.[14–17]

We previously synthesized m-WS particles using rice straw as a source of silica, and mesostructures in $CaSiO_3$ were formed by leaching the calcium ions through acid modification with hydrochloric acid. We also demonstrated that these biocompatible m-WS particles promoted mouse mesenchymal stem-cell proliferation and differentiation.[8] Even though biomaterials or scaffolds are found to be suitable for bone tissue engineering in vitro, these materials may have limitation for in vivo applications due to host response. To our knowledge, no study has been conducted

[1]Department of Biotechnology, School of Bioengineering, SRM University, Kattankulathur, India
[2]Department of Physiology and Pathophysiology, St. Boniface Research Centre, University of Manitoba, Winnipeg, MB, Canada

Corresponding author:
Nagarajan Selvamurugan, Department of Biotechnology, School of Bioengineering, SRM University, Kattankulathur 603 203, India.
Email: selvamurugan.n@ktr.srmuniv.ac.in; selvamn2@yahoo.com

Creative Commons Non Commercial CC-BY-NC: This article is distributed under the terms of the Creative Commons Attribution-NonCommercial 3.0 License (http://www.creativecommons.org/licenses/by-nc/3.0/) which permits non-commercial use, reproduction and distribution of the work without further permission provided the original work is attributed as specified on the SAGE and Open Access pages (https://us.sagepub.com/en-us/nam/open-access-at-sage).

with m-WS particles for in vivo bone formation. Hence, in this study, we tested the bone-forming ability of m-WS particles in rat tibial defect model system.

Materials and methods

Materials

Calcium nitrate tetrahydrate ($Ca(NO_3)_2{\cdot}4H_2O$), sodium hydroxide (NaOH), and hydrochloric acid (HCl) were purchased from Sigma–Aldrich, USA. Carbopol 940 was purchased from Loba Biochemie, India. All other reagents were of analytical grade.

Synthesis of m-WS from rice straw ash

The synthesis of m-WS was carried out as described earlier.[8] These particles exhibited the surface area of 353.48 m^2/g. They had their pore size (R) = 4.5 nm, pore volume = 0.757 cm^2/g, and diameter of 1106 nm. Briefly, rice straw was cleaned and calcinated at 550°C to obtain white rice straw ash (RSA). The calculated amount of the RSA was refluxed in 1 M NaOH for 1 h and sodium silicate solution was obtained by filtration. Equimolar calcium nitrate solution was mixed with sodium silicate to precipitate WS particles. The slurry containing WS:H_2O in the ratio of 1:10 was acid modified by adjusting the pH to 5.5 with 1 M HCl. The precipitate was collected by centrifugation and washed several times with distilled water, and upon drying at 100°C, m-WS particles were obtained and subjected for in vivo studies.

Animals and surgical procedure

A total of 36 male Albino-Wistar rats weighing around 250 g were procured from National Institute of Nutrition (NIN), Hyderabad. All animal experimental procedures were approved by the animal ethical committee, Kovai Medical College and Hospital, Coimbatore, Tamil Nadu, India. A total of three groups (n = 6)—group 1: control, group 2: carbopol-treated, and group 3: carbopol + m-WS-treated animals—were maintained for 2 and 4 weeks in this study. The animals were acclimated in the animal facility for 2 weeks before surgery. The rats were anesthetized with 10% ketamine and 2% xylazine (1:1, 0.1 mL/100 g body weight, intramuscular (i.m.)) and subjected to perforation of the right tibia using a dental drill with 3 mm of diameter under constant saline irrigation (0.9% NaCl). m-WS particles were mixed with an inert gel carbopol to form an adherent paste prior to filling in the defect. The defect was entirely left unfilled (group 1), filled with carbopol (group 2), or filled with m-WS paste (group 3). After second and fourth weeks, the animals were sacrificed by anesthesia, and the tibiae were immediately removed, radiographed, and fixed in neutral 10% buffered formalin for 48 h at room temperature for histological analyses.

Histological processing

The implanted bone/ceramic implants were collected from animals at second and fourth weeks postoperatively. The implanted sections were cut from both normal and implanted area of bone. The implants were washed thoroughly with physiological saline and were fixed in 10% formalin for 7 days. Subsequently, bones were decalcified in 10% ethylenediaminetetraacetic acid (EDTA). The sections were checked regularly for the status of decalcification. The bone parts were identified for its flexibility, transparency, and penetrability by sharp pin to analyze the extent of decalcification. The decalcified tissues were processed in a routine manner, and 6 μm sections were cut and stained with hematoxylin and eosin (H&E) and Masson's trichrome staining, individually. The stained sections were observed for the status of the bone implants and cellular response of host bone to the implants. The stained sections were then viewed under a microscope to visualize the extent of bone formation.

Scanning electron microscope and energy-dispersive spectra analyses

The calcified and unstained thin fixed sections of the bone were subjected to scanning electron microscope (SEM)–energy-dispersive spectra (EDS) analyses for identifying the quality of new bone formed inside the critical-sized tibial defect. The sections were sputter coated with a thin layer of carbon and observed in HR-SEM Quanta 200 FEG Instrument, The Netherlands.

Results and discussion

Critical-sized tibial defect and radiographic assessment

Critical assessment of the osteogenic ability in vivo is crucial for testing biomaterials intended for bone tissue engineering applications.[18–25] With previous evidence emphasizing the osteogenic role of m-WS particles in vitro, in this study, we studied its osteogenic role in vivo in rat-sized tibial defect model system. Dental burr of 3 mm diameter was used to create the defect. The photographic images of the 3-mm circular tibial defect are represented in Figure 1(a) and (b). As mentioned in the experimental section, the defects were entirely left unfilled (group 1), filled with carbopol (group 2), or filled with m-WS and carbopol gel (group 3). Carbopol is an inert gel which does not exert any action on bone formation in the defect. The radiographs of the rat tibial defect filled with m-WS particles–carbopol gel at second and fourth weeks are represented in Figure 2. The result indicated that the tibial bone defect in control group devoid of any implanted material showed a radiolucent gap. The presence of inert gel (carbopol) filled in the drilled hole of the animal group also showed similar radiolucent nature.

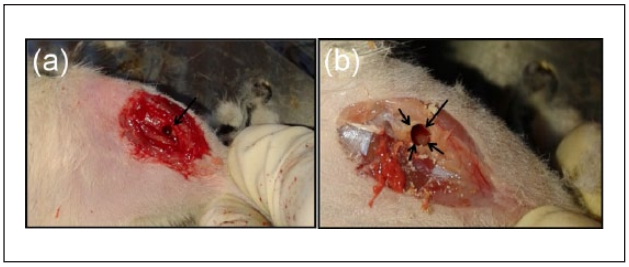

Figure 1. Photographic images of the critical-sized tibial bone defect created in rats. (a) and (b) The defect measured 3 mm in diameter, and spherical dental burr was used to excavate bone tissue. Black arrows indicate the margins of the defect.

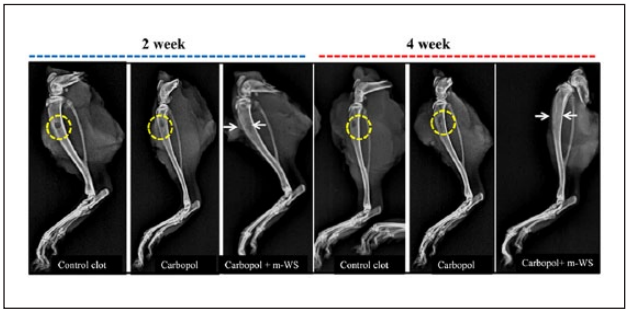

Figure 2. Representative X-ray photographs of the rat tibial defect of control clot (no filler), carbopol, and m-WS + carbopol-healed groups after second and fourth weeks post-implantation. m-WS particles healed the defect at an early period of 2 weeks and extensively bridged the defect after 4 weeks.

Radiographs depicted minimal periosteal reaction and smoothening of cortical bone defect edges in both control and carbopol-treated animal groups. When the tibial bone defect was filled with m-WS particles, there was improved wound closure at the second week, and there was high-dense radio-opacity observed at the fourth week (Figure 2). The area of bone defect changed its shape to oval morphology suggesting the initiation of bone healing. Resorption of the m-WS particles also might have begun as indicated by the smoothening of the round corners of the defect. On implantation, the particles are exposed to tissue fluid resulting in the hydration of m-WS particles and successive formation of silanol groups, followed by the deposition of phosphate and formation of hydroxycarbonate apatite (HCA).[26] The growth of new bone and bridging the defect area in response to m-WS particles is clearly indicative of the biocompatible and osteogenic nature of these particles.

Histological evaluation

Histological assessment was performed to determine the presence of new bone formation in the tibial defect. There was new bone growth (denoted NB) in tibial defect where it was filled with m-WS (Figure 3). The bone layer formed after 2 weeks failed to bridge the defect, but bone growth

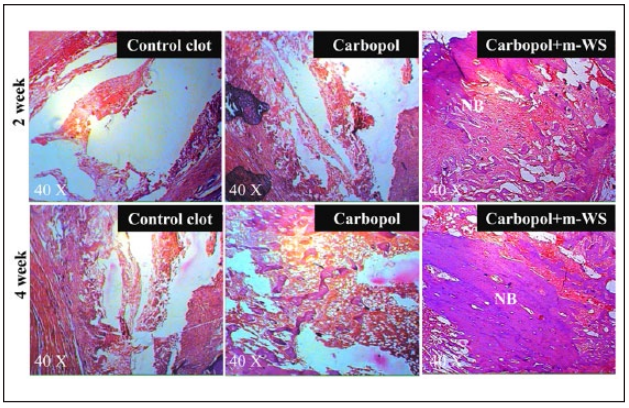

Figure 3. H&E-stained images of the sectioned implants of the tibial defect after second and fourth weeks. No graft material was present in both control and carbopol-treated groups. Bone formation was seen with the inclusion of m-WS particles within the defect. Images were recorded with a 40× objective.
NB: new bone formed.

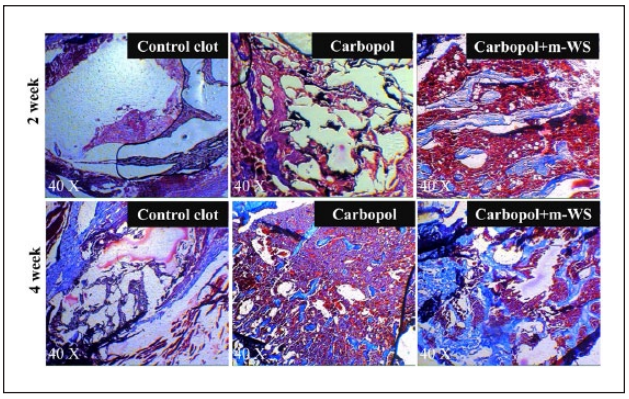

Figure 4. Microscopic images of Masson's trichrome–stained sections of tibial sections after second and fourth weeks post-implantation. Deposition of collagen was high among m-WS-treated groups at both the time periods compared to control and carbopol-treated groups. Images were recorded with 40× objective.

was observed with m-WS particle–treated groups at the end of 4 weeks post-implantation. Bone regeneration and integration with host bone tissue were higher at the end of 4 weeks in response to m-WS particles. In both untreated and carbopol-treated groups at second and fourth weeks, the defect was mostly filled with fibrous connective tissue with less bone filling. Thus, H&E-stained histological analysis of the sectioned implants indicated the formation of new bone and the results are consistent with the radiographic images of the m-WS-treated groups (Figures 2 and 3). Biomaterials with the osteoinductive nature have the ability to guide bone formation from mesenchymal stem cells in the absence of mature bone cells.[27,28] Deposition of collagen was analyzed by Masson's trichrome staining with the sectioned implants, and the images are represented in Figure 4. At the end of both second and fourth

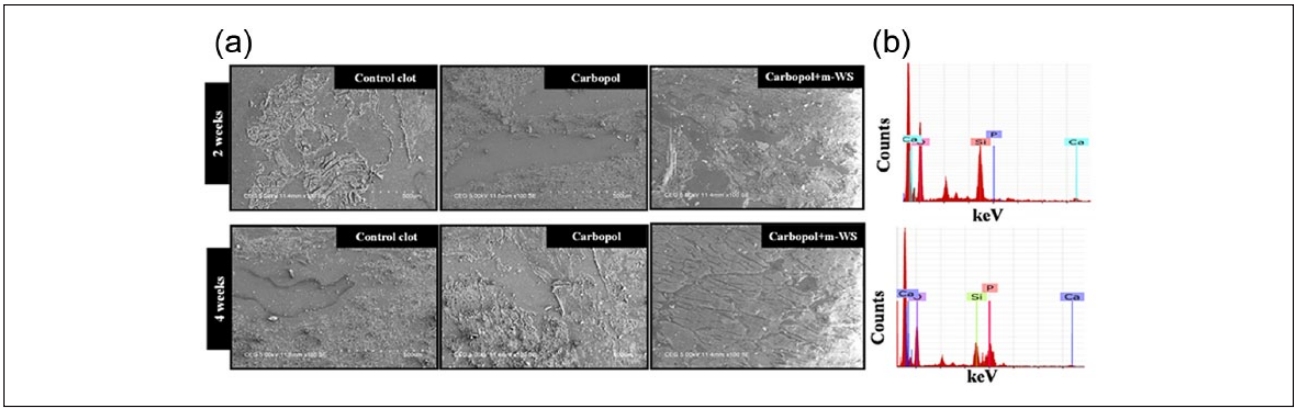

Figure 5. Analysis of apatite formation: (a) SEM analysis of the sectioned implants after second and fourth weeks post-implantation and (b) EDS analysis was performed for the m-WS particle–healed tibial defects. The presence of silicon (Si), calcium (Ca), and phosphorous (P) was observed. Deposition of phosphorous was more at 4 weeks compared to the end of 2 weeks.

weeks, the tibial bone defect filled with m-WS particles showed an increased collagen deposition compared to control and carbopol-treated animal groups (Figure 4). Silicon (Si) is an important regulator of metabolism, collagen synthesis, and bone mineralization.[29–35] It is also involved in osteoblast proliferation, differentiation, and matrix mineralization.[36–38] Silicon has been shown to enhance the proliferation and osteogenic differentiation of osteoblasts and bone marrow stromal cells and thereby promoting bone formation in vivo.[6,39] Increased collagen deposition observed among m-WS particle–treated groups (Figure 4) might be due to the silicon released from the particles in response to body fluids of the in vivo system.

SEM and EDS

The SEM images of the sectioned implants (a) and EDS (b) of m-WS-treated animal groups at second and fourth weeks are shown in Figure 5. The drill hole was almost filled at 4 weeks implantation in m-WS-treated animals (Figure 5(a)). The EDS analysis confirmed the presence of HCA layer in the implanted region (Figure 5(b)). The formation of new bone observed is contributed by the bone-bonding ability of the material with host bone which is an indispensable requirement for functional bone growth.[40] Following implantation of m-WS particles, the surface reaction occurring will result in the formation of bone-like apatite layer. The HCA layer formation is the key for interfacial bonding with host bone which is later covered with new bone tissue. Bone formation on the implanted material is driven by the formed apatite layer through surface reactions in response to the surrounding fluids. Bridging of the tibial defect (Figures 2–5) observed at 4 weeks of implantation could be due to the increased number of silanol groups associated with m-WS particles and increased sites of nucleation. Apatite mineralization of silicon-containing materials is an important phenomenon in the implant bone tissue chemical interaction, which governs the in vivo osteogenesis of such graft materials.[40]

Taken together, in this study, we identified the role of m-WS particles on the induction of new bone growth. Mesopores in the particles and silicon released from them might have fastened the surface reactions leading to the formation of more silanol groups, phosphate deposition, and successive bone tissue ingrowth in vivo.

Conclusion

The in vivo behavior of m-WS particles derived from RSA was investigated in rat critical-sized bone defect model system. From the results, the particles were found to promote deposition of collagen and phosphate and enhance new bone formation at 4 weeks of implantation period in the rat tibia bone defect. Therefore, we suggest that m-WS particles can be used as a potent filling material for bone tissue engineering applications.

Author contribution

S.S. carried out the synthesis of materials, their characterization, and performed the animal studies. N.S. conceived the study and participated in its design and coordination. All authors read and approved the final manuscript.

Declaration of conflicting interests

The author(s) declared no potential conflicts of interest with respect to the research, authorship, and/or publication of this article.

Funding

The author(s) disclosed receipt of the following financial support for the research, authorship, and/or publication of this article: This work was supported by the SRM University and the Council of Scientific and Industrial Research, India (grant nos 37 (1574)/12/EMR-II, 60 (0110)/13/EMR-II to N.S.).

References

1. Hadjidakis DJ and Androulakis II. Bone remodeling. *Ann N Y Acad Sci* 2006; 1092: 385–396.
2. Idaszek J, Zinn M, Obarazanek-Fojt M, et al. Tailored degradation of biocompatible poly(3-hydroxybutyrate-co-3-hydroxyvalerate)/calcium silicate/poly(lactide-co-glycolide) ternary composites: an in vitro study. *Mater Sci Eng C Mater Biol Appl* 2013; 33: 4352–4360.
3. Fei L, Wang C, Xue Y, et al. Osteogenic differentiation of osteoblasts induced by calcium silicate and calcium silicate/β-tricalcium phosphate composite bioceramics. *J Biomed Mater Res B Appl Biomater* 2012; 100: 1237–1244.
4. Ni S, Chang J and Chou L. A novel bioactive porous $CaSiO_3$ scaffold for bone tissue engineering. *J Biomed Mater Res A* 2006; 76: 196–205.
5. Zreiqat H, Ramaswamy Y, Wu C, et al. The incorporation of strontium and zinc into a calcium-silicon ceramic for bone tissue engineering. *Biomaterials* 2010; 31: 3175–3184.
6. Xynos ID, Edgar AJ, Buttery LD, et al. Gene-expression profiling of human osteoblasts following treatment with the ionic products of Bioglass 45S5 dissolution. *J Biomed Mater Res* 2001; 55: 151–157.
7. Ni S, Chang J, Chou L, et al. Comparison of osteoblast-like cell responses to calcium silicate and tricalcium phosphate ceramics in vitro. *J Biomed Mater Res B Appl Biomater* 2007; 80: 174–183.
8. Saravanan S, Vimalraj S, Vairamani M, et al. Role of mesoporous wollastonite (calcium silicate) in mesenchymal stem cell proliferation and osteoblast differentiation: a cellular and molecular study. *J Biomed Nanotechnol* 2015; 11: 1124–1138.
9. Hung CJ, Hsu HI, Lin CC, et al. The role of integrin αv in proliferation and differentiation of human dental pulp cell response to calcium silicate cement. *J Endod* 2014; 40: 1802–1809.
10. Sarkar NK, Caicedo R, Ritwik P, et al. Physicochemical basis of the biologic properties of mineral trioxide aggregate. *J Endod* 2005; 31: 97–100.
11. Bozeman TB, Lemon RR and Eleazer PD. Elemental analysis of crystal precipitate from gray and white MTA. *J Endod* 2006; 32: 425–428.
12. Coleman NJ, Nicholson JW and Awosanya K. A preliminary investigation of the in vitro bioactivity of white Portland cement. *Cement Concrete Res* 2007; 37: 1518–1523.
13. Taddei P, Tinti A, Gandolfi MG, et al. Vibrational study on the bioactivity of Portland cement-based materials for endodontic use. *J Mol Struct* 2009; 924–926: 548–554.
14. Xue W, Bandyopadhyay A and Bose S. Mesoporous calcium silicate for controlled release of bovine serum albumin protein. *Acta Biomater* 2009; 5: 1686–1696.
15. Yan X, Huang X, Yu C, et al. The in-vitro bioactivity of mesoporous bioactive glasses. *Biomaterials* 2006; 27: 3396–3403.
16. Li X, Shi J, Zhu Y, et al. A template route to the preparation of mesoporous amorphous calcium silicate with high in vitro bone-forming bioactivity. *J Biomed Mater Res B Appl Biomater* 2007; 83: 431–439.
17. De Aza PN, Luklinska ZB, Martinez A, et al. Morphological and structural study of pseudowollastonite implants in bone. *J Microsc* 2000; 197: 60–67.
18. Schliephake H, Knebel JW, Aufderheide M, et al. Use of cultivated osteoprogenitor cells to increase bone formation in segmental mandibular defects: an experimental pilot study in sheep. *Int J Oral Maxillofac Surg* 2001; 30: 531–537.
19. Shang QX, Wang Z, Liu W, et al. Tissue-engineered bone repair of sheep cranial defects with autologous bone marrow stromal cells. *J Craniofac Surg* 2001; 12: 586–593.
20. Wu W, Chen X, Mao T, et al. Bone marrow-derived osteoblasts seeded into porous beta-tricalcium phosphate to repair segmental defect in canine's mandibula. *Ulus Travma Acil Cerrahi Derg* 2006; 12: 268–276.
21. He Y, Zhang ZY, Zhu HG, et al. Experimental study on reconstruction of segmental mandible defects using tissue engineered bone combined bone marrow stromal cells with three-dimensional tricalcium phosphate. *J Craniofac Surg* 2007; 18: 800–805.
22. Kon E, Muraglia A, Corsi A, et al. Autologous bone marrow stromal cells loaded onto porous hydroxyapatite ceramic accelerate bone repair in critical-size defects of sheep long bones. *J Biomed Mater Res* 2000; 49: 328–337.
23. Petite H, Viateau V, Bensaïd W, et al. Tissue-engineered bone regeneration. *Nat Biotechnol* 2000; 18: 959–963.
24. Bruder SP, Kraus KH, Goldberg VM, et al. The effect of implants loaded with autologous mesenchymal stem cells on the healing of canine segmental bone defects. *J Bone Joint Surg Am* 1998; 80: 985–996.
25. Viateau V, Guillemin G, Bousson V, et al. Long-bone critical-size defects treated with tissue-engineered grafts: a study on sheep. *J Orthop Res* 2007; 25: 741–749.
26. Magallanes-Perdomo M, Luklinska ZB, De Aza AH, et al. Bone-like forming ability of apatite-wollastonite glass ceramic. *J Eur Ceram Soc* 2011; 31: 1549–1561.
27. Habibovic P and De Groot K. Osteoinductive biomaterials—properties and relevance in bone repair. *J Tissue Eng Regen Med* 2007; 1: 25–32.
28. Barradas AM, Yuan H, Van Blitterswijk CA, et al. Osteoinductive biomaterials: current knowledge of properties, experimental models and biological mechanisms. *Eur Cell Mater* 2011; 21: 407–429.
29. Carlisle EM. Silicon: a requirement in bone formation independent of vitamin D1. *Calcif Tissue Int* 1981; 33: 27–34.
30. Nielsen FH and Sandstead HH. Are nickel, vanadium, silicon, fluorine, and tin essential for man? A review. *Am J Clin Nutr* 1974; 27: 515–520.
31. Carlisle EM. Silicon: a possible factor in bone calcification. *Science* 1970; 167: 279–280.
32. Schwarz K and Milne DB. Growth-promoting effects of silicon in rats. *Nature* 1972; 239: 333–334.
33. Hott M, de Pollak C, Modrowski D, et al. Short-term effects of organic silicon on trabecular bone in mature ovariectomized rats. *Calcif Tissue Int* 1993; 53: 174–179.
34. Macdonald HM, Hardcastle AC, Jugdaosingh R, et al. Dietary silicon interacts with oestrogen to influence bone health: evidence from the Aberdeen prospective osteoporosis screening study. *Bone* 2012; 50: 681–687.
35. Martin KR. The chemistry of silica and its potential health benefits. *J Nutr Health Aging* 2007; 11: 94–98.

36. Zou S, Ireland D, Brooks RA, et al. The effects of silicate ions on human osteoblast adhesion, proliferation, and differentiation. *J Biomed Mater Res B Appl Biomater* 2009; 90: 123–130.
37. Lehman G, Cacciotti I, Palmero P, et al. Differentiation of osteoblast and osteoclast precursors on pure and silicon-substituted synthesized hydroxyapatites. *Biomed Mater* 2012; 7: 055001.
38. Wang B, Sun J, Qian S, et al. Proliferation and differentiation of osteoblastic cells on silicon-doped TiO(2) film deposited by cathodic arc. *Biomed Pharmacother* 2012; 66: 633–641.
39. Xynos ID, Edgar AJ, Buttery LD, et al. Ionic products of bioactive glass dissolution increase proliferation of human osteoblasts and induce insulin-like growth factor II mRNA expression and protein synthesis. *Biochem Biophys Res Commun* 2000; 276: 461–465.
40. Xu S, Lin K, Wang Z, et al. Reconstruction of calvarial defect of rabbits using porous calcium silicate bioactive ceramics. *Biomaterials* 2008; 29: 2588–2596.